A permeability transition in liver mitochondria and liposomes induced by α,ω-dioic acids and Ca^{2+}

Mikhail V. Dubinin · Victor N. Samartsev · Maxim E. Astashev · Alexey S. Kazakov · Konstantin N. Belosludtsev

Abstract The article examines the molecular mechanism of the Ca^{2+}-dependent cyclosporin A (CsA)-insensitive permeability transition in rat liver mitochondria induced by α,ω-dioic acids. The addition of α,ω-hexadecanedioic acid (HDA) to Ca^{2+}-loaded liver mitochondria was shown to induce a high-amplitude swelling of the organelles, a drop of membrane potential and the release of Ca^{2+} from the matrix, the effects being insensitive to CsA. The experiments with liposomes loaded with sulforhodamine B (SRB) revealed that, like palmitic acid (PA), HDA was able to cause permeabilization of liposomal membranes. However, the kinetics of HDA- and PA-induced release of SRB from liposomes was different, and HDA was less effective than PA in the induction of SRB release. Using the method of ultrasound interferometry, we also showed that the addition of Ca^{2+} to HDA-containing liposomes did not change the phase state of liposomal membranes—in contrast to what was observed when Ca^{2+} was added to PA-containing vesicles. It was suggested that HDA/Ca^{2+}- and PA/Ca^{2+}-induced permeability transition occurs by different mechanisms. Using the method of dynamic light scattering, we further revealed that the addition of Ca^{2+} to HDA-containing liposomes induced their aggregation/fusion. Apparently, these processes result in a partial release of SRB due to the formation of fusion pores. The possibility that this mechanism underlies the HDA/Ca^{2+}-induced permeability transition of the mitochondrial membrane is discussed.

Abbreviations

CsA	Cyclosporin A
HDA	α,ω-Hexadecanedioic acid
PA	Palmitic acid
TDA	α,ω-Tetradecanedioic acid
SRB	Sulforhodamine B
TPP$^+$	Cation tetraphenylphosphonium
LUV	Large unilamellar vesicle
TX-100	Triton X-100
DPPC	1,2-Dipalmitoylphosphatidylcholine

M. V. Dubinin (✉) · V. N. Samartsev
Mari State University, pl. Lenina 1, Yoshkar-Ola,
Mari El 424001, Russia
e-mail: dubinin1989@gmail.com

M. V. Dubinin · M. E. Astashev · K. N. Belosludtsev
Institute of Theoretical and Experimental Biophysics RAS,
Institutskaya 3, Pushchino, Moscow Region 142290, Russia

M. E. Astashev
Institute of Cell Biophysics RAS, Institutskaya 3, Pushchino,
Moscow Region 142290, Russia

A. S. Kazakov
Institute for Biological Instrumentation RAS, Institutskaya 7,
Pushchino, Moscow Region 142290, Russia

Introduction

α,ω-Dioic acids are formed in the liver cells as a result of ω-oxidation of the corresponding monocarboxylic fatty acids (Sanders et al. 2005; Reddy and Rao 2006; Wanders et al. 2011). Under normal physiological conditions, only 5–10 % of monocarboxylic fatty acids are metabolized through this pathway. However, the level of α,ω-dioic acids in liver cells substantially increases with some pathologies (obesity, starvation, diabetes mellitus), as well as various disorders of the monocarboxylic fatty acid metabolism (Reddy and Rao 2006; Wanders et al. 2011). In Reye's

syndrome, which is characterized by acute encephalopathy and infiltration of fat into liver cells (Tonsgard 1986), the level of α,ω-dioic acids in the blood serum of children rises to 55 % of total fatty acids. Most of these α,ω-dioic acids (up to 90 %) are long-chain acids (C16–C18), and their concentration in the serum can reach 0.5 mM (Tonsgard 1986). It has also been shown that ω-oxidation of free fatty acids (FFAs) in liver cells is significantly enhanced under the effect of some xenobiotics and chronic influence of ethanol (Kundu et al. 1991; Orellana et al. 1998). In addition, accumulation of α,ω-dioic acids in liver cells is known to occur in ground squirrels at the late stages of their hibernation (Nelson et al. 2009), although nothing is known about the biological role of the phenomenon and its consequences for the hibernating animal. It is also unclear how much the increase in the level of α,ω-dioic acids in the liver tissue, which is observed at various pathologies, is associated with the functional disorders of this vital organ.

At present, biologists consider a few types of cell death, which differ according to both morphological manifestations and biochemical mechanisms. In all cases, however, the central role is played by the mitochondria, which integrate many intracellular signal pathways leading to cell death (Malhi et al. 2010; Kroemer et al. 2007; Rasola and Bernardi 2011). One of the mitochondria-related steps in the complex mechanism of cell death is the transition in the nonspecific permeability of the inner mitochondrial membrane, which is induced by Ca^{2+}. Following the permeability transition is the impairment of the energy-transducing functions of mitochondria (first of all, ATP synthesis) as well as the release of the so-called apoptogenic proteins—cytochrome c, apoptosis-inducing factor, endonuclease G, etc.—from the intermembrane space into the cytoplasm (Kroemer et al. 2007; Rasola and Bernardi 2011).

It is well known that free monocarboxylic fatty acids are effective natural inductors of nonspecific permeability transition in the inner mitochondrial membrane (Sultan and Sokolove 2001a, b; Mironova et al. 2004; Belosludtsev et al. 2005, 2006; Di Paola and Lorusso 2006). The "classical" mechanism of permeability transition implies that fatty acids interact with one of the components of the putative pore complex: the ADP/ATP antiporter. In this case, the effect of fatty acids manifests itself only in the presence of Ca^{2+} (other divalent cations are not effective) and is suppressed with CsA (Sultan and Sokolove 2001a). At the same time, it is established that palmitic and some other saturated fatty acids are able to open a nonspecific pore in liver mitochondria that is insensitive to CsA. In this case, Ca^{2+} can be replaced with other divalent cations. Unsaturated fatty acids cannot open this pore (Sultan and Sokolove 2001a, b; Mironova et al. 2004; Belosludtsev et al. 2005, 2006). The formation of such a pore was also demonstrated on liposomal membranes (Agafonov

et al. 2003, 2007). This enabled us to suggest that the CsA-insensitive pore induced by palmitic and other saturated fatty acids in the inner mitochondrial membrane had a lipid nature. The opening of this pore seems to occur by the mechanism of chemotropic phase transition in the lipid bilayer; it is based on the formation and subsequent segregation of Ca^{2+} or Sr^{2+} complexes with fatty acids into solid membrane domains (Agafonov et al. 2007).

We have recently shown that α,ω-dioic acids are able to open a "non-classical" CsA-insensitive pore in Ca^{2+}- or Sr^{2+}-loaded liver mitochondria, with α,ω-hexadecanedioic acid (HDA) being the most effective inducer. Necessary requirements for the pore opening is energization of the organelles and presence of Ca^{2+} or Sr^{2+} in their matrix (Dubinin et al. 2013, 2014).

In the present work, we continue to study the role of α,ω-dioic acids as inducers of the CsA-insensitive Ca^{2+}-dependent nonspecific permeability transition in liver mitochondria. In addition, to elucidate the molecular mechanism of this phenomenon, we examine the effect of HDA on the membrane of liposomes in the presence of Ca^{2+}. The effects of HDA are compared to the effects of α,ω-tetradecanedioic acid (TDA), which has a shorter acyl chain. The data obtained are considered evidence of the ability of α,ω-dioic acids to induce Ca^{2+}-dependent CsA-insensitive permeability transition in both mitochondrial and liposomal membranes.

Materials and methods

Materials

Medium components, all inorganic chemicals, fatty acids, sulforhodamine B, tetraphenyl phosphonium, cyclosporn A and lecithin were purchased from Sigma-Aldrich; DPPC was purchased from Avanti Polar Lipids.

Preparation of mitochondria

Experiments were conducted on mitochondria isolated from the liver of Wistar rats (animal weight was 210–250 g) using a convenient technique of differential centrifugation (Markova et al. 1999). The isolation medium contained 250 mM sucrose, 1 mM EGTA and 5 mM Hepes-Tris buffer (pH 7.4). The mitochondrial protein concentration was determined by the biuret method with BSA used as standard.

Mitochondrial swelling was detected by changes in the optical density of the mitochondrial suspension (A) at 540 nm using a KFK-3-01 spectrometer (ZOMZ, Russia) in a 4-ml cell and at 25 °C. The incubation medium contained 200 mM sucrose, 20 mM KCl, 20 μM EGTA,

5 mM succinic acid and 10 mM Hepes-Tris buffer (pH 7.4). Also, 2 µM rotenone was added to the cuvette just before measurements.

The concentration of Ca^{2+} ions in the incubation medium was determined with a Ca^{2+}-selective electrode. $\Delta\psi$ was estimated by following the distribution of tetraphenylphosphonium (TPP^+) across the mitochondrial membrane; in this case, the incubation medium was supplemented with 1.6 µM TPP^+. The concentration of TPP^+ was measured with a TPP^+-sensitive electrode (Kamo et al. 1979). The changes in TPP^+ and Ca^{2+} concentrations were recorded simultaneously in a 1.5-ml cell at constant stirring and thermostating (25 °C) using a Record-4 USB original multi-channel electrometrical system.

Preparation of large unilamellar vesicles

Large unilamellar vesicles (LUVs) were obtained by a conventional extrusion technique. Dry egg phosphatidylcholine (lecithin) (0.75 mg) was hydrated in 0.75 ml of buffer for several hours with periodic stirring in a vortex mixer. The buffer contained 10 mM Tris-HCl (pH 8.5), 40 mM KCl and 50 µM EGTA. After five cycles of freezing/thawing at −20/+30 °C, the suspension of multilamellar liposomes was pressed 11 times through a 0.1-µm polycarbonate membrane using an Avanti microextruder (Avanti Polar Lipids, Birmingham, AL). All operations (excluding the freezing/thawing procedure) were carried out at room temperature.

Measurement of permeabilization of SRB-loaded liposomes

SRB-loaded LUVs were prepared from egg phosphatidylcholine by a procedure similar to that described above except that (1) the buffer for lipid hydration contained 50 mM SRB instead of 40 mM KCl and (2) after extrusion liposomes were applied on a Sephadex G-50 column to remove the external SRB. The buffer for gel filtration contained 10 mM Tris-HCl (pH 8.5), 50 µM EGTA and 40 mM KCl.

The release of SRB from LUVs was detected by the increase in fluorescence due to the dissociation of SRB excimers after the dilution of dye in the external medium. SRB fluorescence was measured at 25 °C using an Ocean Optics USB 2000 spectrofluorimeter (excitation wavelength, 565 nm; emission wavelength, 586 nm). The fluorescence of SRB was found to be stable for hours and had a linear dependence on the SRB concentration in the range 10^{-8}–10^{-6} M. In our experiments, SRB-loaded LUVs were added to 2 ml of buffer (10 mM Tris-HCl, 50 µM EGTA and 40 mM KCl, pH 8.5), and their fluorescence was measured before and after various additions. Each experiment

was concluded with the final estimation of maximal fluorescence observed upon the total release of SRB from LUVs, the latter being achieved by the addition of 0.1 % Triton X-100 (TX-100). The quantity of LUVs to be added to a sample was adjusted so that the maximal fluorescence was always at the same level. The molar phospholipid concentration in samples measured by the modified Bartlett technique (Bartlett 1959; Kates 1972) was 30–50 µM. Free fatty acids were added to samples as ethanol solutions, with the final concentration of ethanol never exceeding 1 %. At this concentration, ethanol did not cause any release of SRB from LUVs. The release of SRB from LUVs upon the effect of an acting factor (i.e., a chemical or a combination of chemicals) was calculated as a percentage of total SRB entrapped in the LUVs: $R = \frac{k_F F_F - F_B}{0.88 \times F_T - F_B} \times 100\,\%$, where R is the release of SRB from the LUV induced by an acting factor; F_B is the base fluorescence level observed after the addition of LUVs; F_F is the fluorescence after the effect of an acting factor; F_T is the fluorescence upon the total release of SRB from LUVs after the addition of TX-100; k_F is the correction coefficient for F_F—it was used when the fluorescence of SRB was affected by the acting factor itself (in most cases, k_F was equal to 1); 0.88 is a value of the correction coefficient for TX-100, which was found to increase SRB fluorescence.

Acoustic measurements

The parameters of the main phase transition in the membrane of dipalmitoylphosphatidylcholine (DPPC) LUVs were measured with a temperature-scanning differential ultrasonic fixed-length interferometer (Kharakoz et al. 2007; Astashev et al. 2014). The measured quantity was the relative change in sound velocity and absorption caused by the dispersed lipid of the concentration, c: $[U] = (u - u_0/u_0 c)$ and $[A] = (\alpha\lambda - \alpha_0\lambda_0)/c$. Scan rates were ∼0.3 K/min on cooling runs. LUVs were obtained as described above except that (1) DPPC was used instead of egg phosphatidylcholine, (2) the concentration of DPPC in samples was higher (4.07 mM), and (3) all operations were carried out at 45 °C. The medium contained 10 mM Tris-HCl buffer (pH 8.5), 50 µM EGTA and 40 mM KCl. HDA was added to the dispersion of DPPC as an ethanolic solution.

Dynamic light scattering

Particle size of the LUV was measured by dynamic light scattering at 25 °C Zetasizer Nano ZS (Malvern Instruments Ltd.). The back-scattered light from a 4-mW He/Ne laser (632.8 nm) was collected at an angle of 173°. LUVs were prepared as described above for the preparation of LUV particles. The molar phospholipid concentration in

samples was 50 μM. The medium contained 10 mM Tris-HCl buffer (pH 8.5), 50 μM EDTA and 40 mM KCl. HDAs were added to samples as ethanol solutions, with the final concentration of ethanol never exceeding 1 %. The acquisition time for a single autocorrelation function was 100 s. The resulting autocorrelation functions are averaged values from ten measurements. The volume-weighted size distributions were calculated using the following parameters: the refractive index of the solution, 1.330; refractive index of particles, 1.459 (refractive index of lecithin); a viscosity value of the solution, 0.8882 cP.

Statistical analysis

The data were analyzed using the Graph Pad Prizm 5 and Excel software and presented as mean ± SEM of 3–5 experiments. Statistical differences between data points were determined by a two-tailed t test.

Results and discussion

In the experiments, we used HDA as a representative of the homologous series of α,ω-dioic acids. It is known that HDA is formed in the cells of liver as a result of ω-oxidation of palmitic acid (Ferdinandusse et al. 2004), one of the most abundant natural fatty acids (Wojtczak and Schönfeld 1993). As was shown earlier (Dubinin et al. 2013) and is confirmed in the present work (Fig. 1), the addition of HDA to the suspension of Ca^{2+}-loaded mitochondria leads to a substantial decrease of absorbance in both the presence and absence of CsA. This indicates swelling of the organelles as a result of the CsA-insensitive transition in the nonspecific permeability of the inner membrane (Sultan and Sokolove 2001a, b). In addition, the permeability transition induced by HDA in Ca^{2+}-loaded liver mitochondria leads to the efflux of Ca^{2+} from the mitochondrial matrix and the fall of the membrane potential (Fig. 2).

It was shown earlier that, apart from inducing a Ca^{2+}-dependent permeability transition in mitochondria (Belosludtsev et al. 2005), palmitic and some other saturated monocarboxylic fatty acids are able to permeabilize artificial membranes (Agafonov et al. 2003, 2007). In this work, we present data showing that, like its predecessor palmitic acid, HDA can induce a leak of the fluorescent dye SRB from unilamellar liposomes upon the addition of Ca^{2+} (Fig. 3). However, the kinetics of the HDA-induced SRB release differ from those observed in the case of palmitic acid. As shown in Fig. 3, the addition of PA and Ca^{2+} to liposomes results in a sharp increase in the SRB fluorescence. Fluorescence jumps to a new stable level immediately after the addition of Ca^{2+}. In case of HDA-containing liposomes, the addition of Ca^{2+} leads to a slow growth of
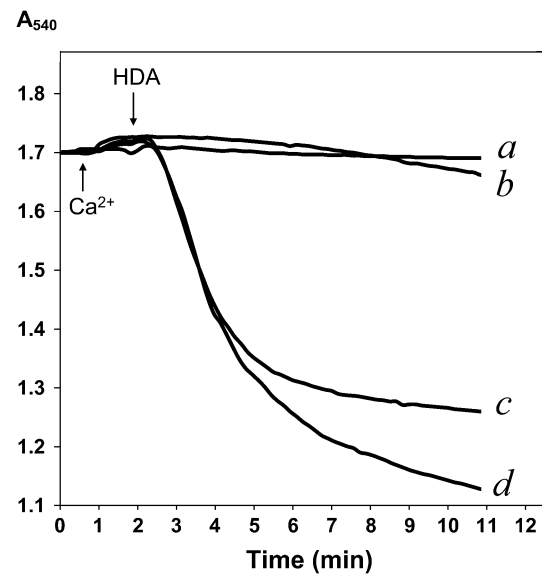

Fig. 1 Effect of HDA (**a**), Ca^{2+} (**b**) and their combined effect on the kinetics of light-scattering changes of the liver mitochondrial suspension in the presence (**c**) or absence (**d**) of 1 μM CsA. The incubation medium contained 200 mM sucrose, 20 mM KCl, 20 μM EGTA, 5 mM succinic acid and 10 mM Hepes-Tris (pH 7.4). The concentration of mitochondrial protein was 0.8 mg/ml. Additions: 200 μM calcium chloride (Ca^{2+}); 20 μM HDA; 1 μM CsA (not shown). Similar results were obtained in three independent experiments
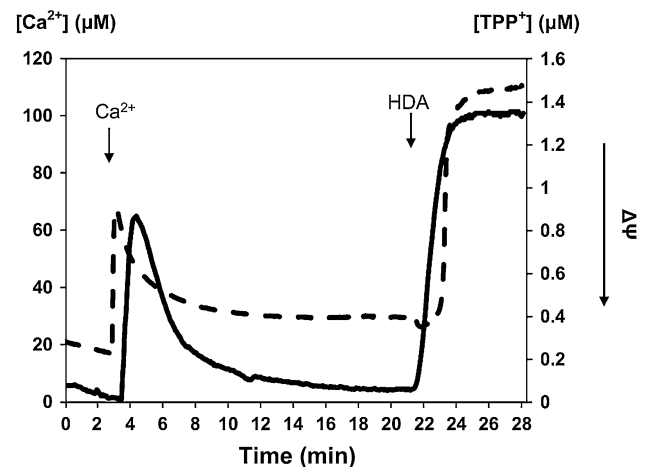

Fig. 2 Changes in the $\Delta\psi$ (*dashed line*) and Ca^{2+} concentration (*solid line*) in response to the addition of Ca^{2+} and HDA. The concentration of mitochondrial protein is 1.5 mg/ml. The medium composition is the same as in Fig. 1

fluorescence, and it takes a few minutes until it reaches the plateau. It should be noted that alone neither fatty acids nor Ca^{2+} caused a leak of SRB from liposomes (Fig. 3).

The dependences of the SRB release from liposomes on the concentration of HDA and Ca^{2+} are given in Figs. 4 and 5 respectively. As seen in the figures, the release
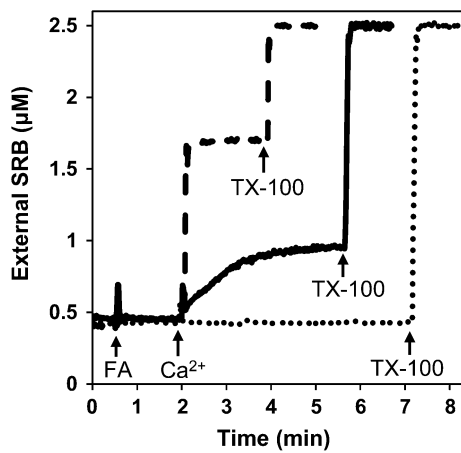
Fig. 3 Release of SRB from lecithin liposomes upon the addition of fatty acids (FAs) and Ca^{2+}. Medium composition: 10 mM Tris-HCl; 50 μM EGTA; 40 mM KCl (pH 8.5). Common additions: 0.1 % TX-100. *Dashed line* 50 μM PA + 1 mM $CaCl_2$ + 0.1 % TX-100, *solid line* 50 μM HDA + 1 mM $CaCl_2$ + 0.1 % TX-100, *dotted line* 1 mM $CaCl_2$ + 0.1 % TX-100

Fig. 5 Dependence of SRB release from lecithin liposomes on the concentration of Ca^{2+}. Medium composition: 10 mM Tris-HCl; 50 μM EGTA; 40 mM KCl (pH 8.5). Common additions: 0.1 % TX-100; 50 μM PA (or HDA). *Dashed line* PA; *solid line* HDA. The data are represented as mean ± SEM ($n = 3$)
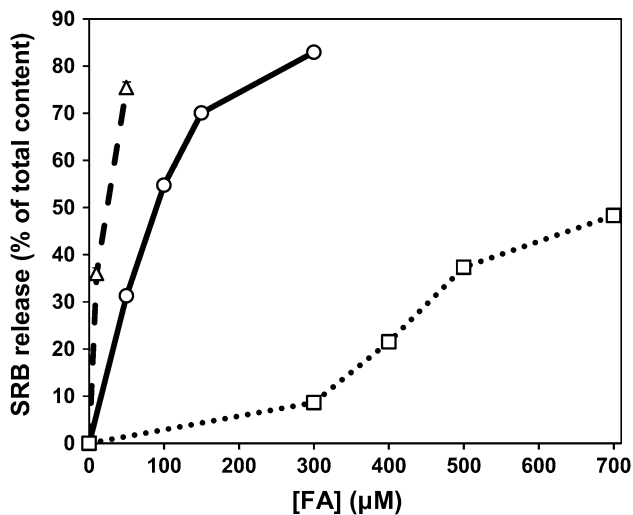

Fig. 4 Dependence of SRB release from lecithin liposomes on the concentration of FA. Medium composition: 10 mM Tris-HCl; 50 μM EGTA 40 mM KCl (pH 8.5). Common additions: 0.1 % TX-100; 1 mM $CaCl_2$. *Dashed line* PA; *solid line* HDA; *dotted line* TDA. The data are represented as mean ± SEM ($n = 3$)

depends on the concentration of both HDA and Ca^{2+}, reaching maximal values at concentrations of HDA about 300 μM and Ca^{2+} of about 2 mM. Thus, as an inducer of permeability changes, HDA is second to palmitic acid. We also compared the effect of HDA with that of TDA, which is shorter than HDA by two carbons. As seen in Fig. 4, TDA is far less effective than HDA regarding the ability to induce Ca^{2+}-dependent membrane permeabilization. Hence, as the number of carbons in its acyl chain decreases, the effectiveness of an α,ω-dioic acid drops
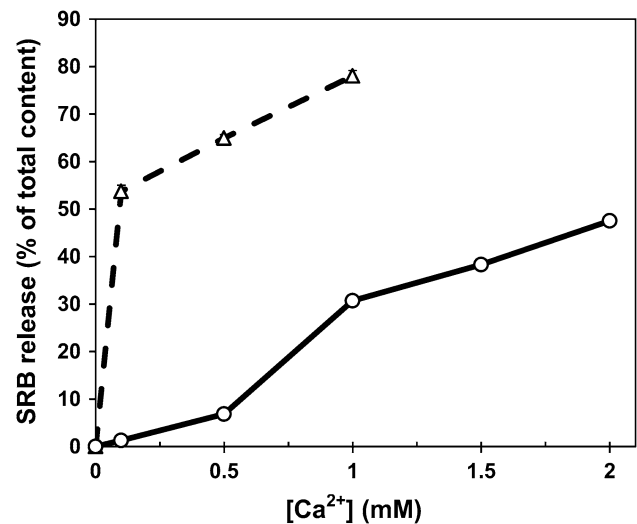
significantly. Earlier, we showed a similar dependence on the acyl chain length of α,ω-dioic acids in regard to their effectiveness as inducers of the permeability transition in liver mitochondria (Dubinin et al. 2013). The longer the acyl chain of a fatty acid is, the higher its lipid/water partition coefficient. One can, therefore, suppose that the effectiveness of Ca^{2+}-dependent permeabilization of both liposomal and mitochondrial membranes will depend on how fast and easy the process of distribution of a fatty acid in the lipid bilayer is.

As is known, the interaction of fatty acids with Ca^{2+} depends on the pH of the buffer. In an alkalescent medium, fatty acids are presumably in the anion form, which will facilitate their interaction with Ca^{2+} (Mironova et al. 2001). As shown earlier, palmitic acid, which binds Ca^{2+} with high affinity, mainly causes Ca^{2+}-dependent membrane permeabilization in the alkalescent region (pH 7.5–8.5) (Agafonov et al. 2003). As seen in Fig. 6, the HDA/Ca^{2+}-induced release of SRB from liposomes also depends on the pH of the medium. At the same time, the maximal HDA/Ca^{2+}-induced SRB release was observed in the alkaline region (pH 9.0–10.0). The difference in the optimal pH value for the effects of mono- and dioic fatty acids is probably determined by the difference in their pK_a.

The data obtained on liposomes and mitochondria indicate that, interacting with Ca^{2+} ions, HDAs are able to permeabilize membranes, and these permeability changes have a lipid nature. As in the case with monocarboxylic fatty acids, the pH optimum of membrane permeabilization lies in the alkaline region, and the effectiveness of dioic fatty
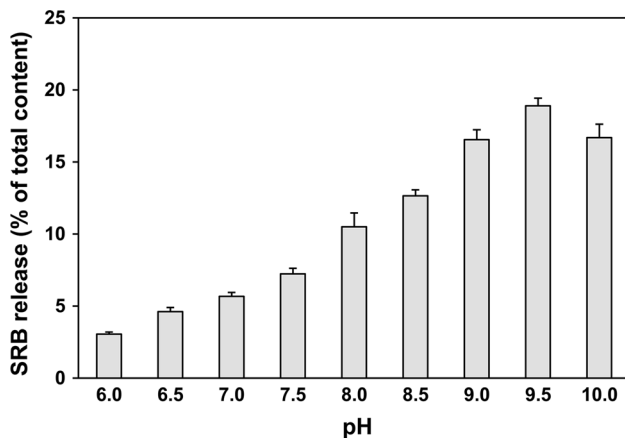
Fig. 6 pH-dependence of SRB release from liposomes induced by the sequential addition of HDA and Ca^{2+}. Medium composition, common additions and the addition order are as in Fig. 3. Concentration of HDA-50 μM, $CaCl_2$-1 mM. The data are represented as mean ± SEM ($n = 3$)

acids also grows as their chain length increases. On the other hand, different kinetics of palmitate/Ca^{2+}-and HDA/Ca^{2+}-induced permeabilization of liposomes and mitochondria allow us to suppose that the mechanisms of permeabilization are different for mono- and dioic fatty acids.

As was shown in the earlier works (Agafonov et al. 2003, 2007), palmitate/Ca^{2+}-induced permeabilization of mitochondria and liposomes is based on the phenomenon of chemotropic phase transition. It was demonstrated that, being added to the suspension of DPPC liposomes, palmitic acid increased the temperature of the lipid phase transition, whereas the subsequent addition of Ca^{2+} returned the phase transition point to the initial value (Agafonov et al. 2007; Belosludtsev et al. 2014). In the present work, we examined the effect of HDA and Ca^{2+} on the phase state of liposomal membranes using the method of ultrasound interferometry. Figure 7 shows the temperature dependence of specific sound velocity and specific sound absorption by DPPC in the presence of HDA and Ca^{2+}. The sharp increase in absorption and decrease in velocity reflect a change in the phase state of lipid in the membrane (raising temperature results in the transition from gel to liquid-crystalline state). The S-shaped region of the specific sound velocity curve (Fig. 7b) indicates the main (temperature) phase transition. For DPPC, the temperature of gel-to-liquid-crystal phase transition is 41.5 °C. HDA increases the temperature of the lipid phase transition to 43.5 °C, making the membrane more rigid. This effect of HDA is similar to that of palmitic acid. At the same time, the addition of Ca^{2+} to HDA-containing liposomes does not cause changes in the phase state of the membrane—in contrast to what was observed for palmitic acid. After the addition of Ca^{2+}, the shapes of the curves remain the
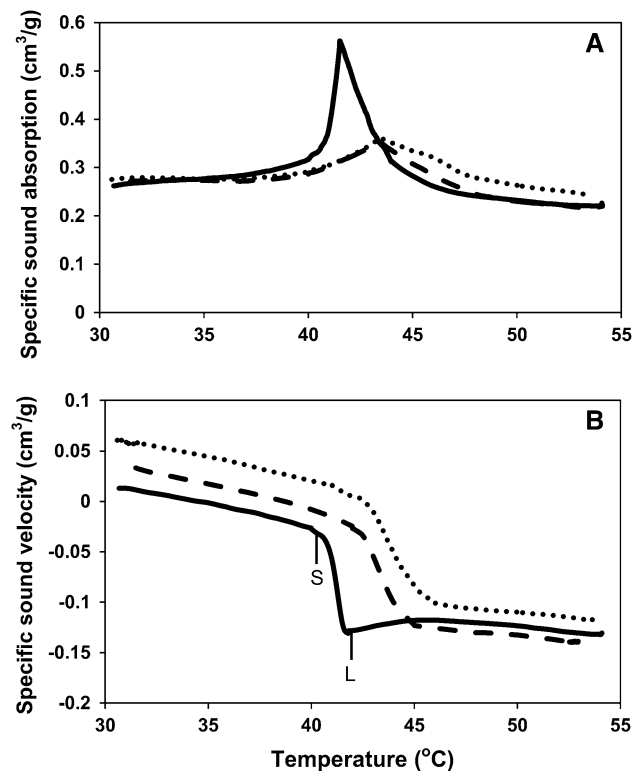

Fig. 7 Effect of Ca^{2+} on the phase behavior of a DPPC/HDA mixture. **a** Temperature dependence of specific sound absorption in the cell containing DPPC liposomes. **b** Temperature dependence of specific sound velocity in the cell containing DPPC liposomes. The points of solidus (*S*) and liquidus (*L*) are defined as the points of maximal curvature. *Solid line* liposomes (4.07 mM DPPC); *dashed line* liposomes (4.07 mM DPPC) + 1 mM HDA; *dotted line* liposomes (4.07 mM DPPC) + 1 mM HDA + 1 mM Ca^{2+}

same as they were in the presence of HDA alone. Hence, it is unlikely that complexes of HDA with Ca^{2+} form solid domains in the membrane. Therefore, HDA/Ca^{2+}-induced permeabilization of mitochondria and liposomes seems to be based on a mechanism that differs from the mechanism of chemotropic phase transition described earlier for palmitic acid.

Permeabilization of lipid membranes by HDA and Ca^{2+} could be explained by the detergent effect of HDA, since its working concentration is relatively high. In this case, a part of the liposomes should be dispersed. To test this supposition, we examined the effect of HDA and Ca^{2+} on the size of vesicles by the method of dynamic light scattering. As seen in Fig. 8, the average hydrodynamical diameter of control liposomes under those conditions was 140 nm. The addition of HDA to the suspension of liposomes did not result in the change of the average size of vesicles. However, the subsequent addition of Ca^{2+} led to a substantial (up to 520 nm) increase of the average hydrodynamical diameter of liposomes. It should
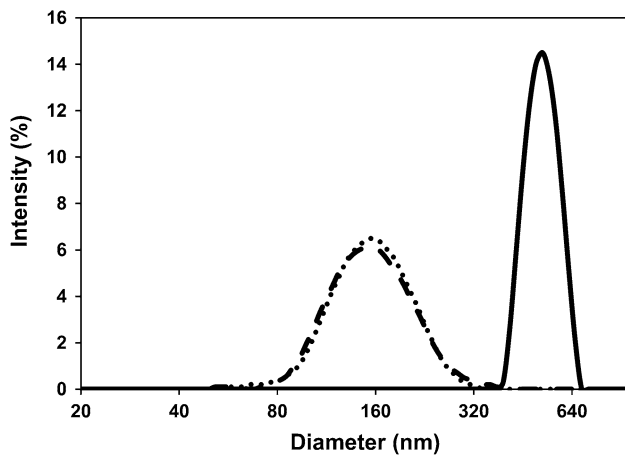
Fig. 8 The distribution of liposomes over their size. Medium composition: 10 mM Tris-HCl; 50 μM EGTA; 40 mM KCl (pH 8.5). *Dotted line* liposomes (50 μM lecithin); *dashed line* liposomes (50 μM lecithin) + 75 μM HDA; *solid line* liposomes (50 μM lecithin) + 75 μM HDA + 1 mM Ca^{2+}

be noted that the addition of 1–2 mM Ca^{2+} to the suspension of control liposomes (without HDA) did not cause changes in their size, which corresponds to the literature data on the effect of Ca^{2+} on fusion and aggregation of lipid vesicles (Papahadjopoulos et al. 1990). The addition of the non-ionic surfactant Triton X-100 resulted in the appearance of small vesicles (about 5 nm) (data not shown).

The data obtained indicate that the cause of HDA/Ca^{2+}-induced SRB release from liposomes may be aggregation and/or fusion of vesicles. It is known that some amphiphilic compounds can initiate fusion and aggregation of liposomes in the presence of Ca^{2+}. For example, unsaturated fatty acids were shown to stimulate fusion of liposomes in the presence of high Ca^{2+} concentrations (Wilschut et al. 1992; Belosludtsev et al. 2014). The results of the present work indicate that HDA is able to induce Ca^{2+}-dependent aggregation/fusion and permeabilization of liposomes as well. It is known that the processes of fusion and aggregation depend on the lipid composition of the membrane and are often accompanied by destabilization of the bilayer and the appearance of pre-fusion structures (a semi-fusion structure, fusion pore, etc.) (Chernomordik and Kozlov 2003, 2008; Lentz et al. 2000; Jackson and Chapman 2008). It is possible that these rearrangements of the liposomal membrane lead to the release of SRB from liposomes.

It can be suggested that the mechanism of HDA/Ca^{2+}-dependent permeability transition described above is realized in liver mitochondria. Earlier we established (Dubinin et al. 2013, 2014) that the necessary condition for the induction of CsA-insensitive permeability transition in

mitochondria by HDA is the accumulation of Ca^{2+} in the matrix of the organelles. It seems that the formation of HDA/Ca^{2+} complexes in the inner monolayer of the inner membrane may lead to its spontaneous bending and protrusion toward the outer membrane. As a result, the two membranes may come into close contact and fuse, with the formation of a fusion pore and the subsequent swelling of mitochondria. It is possible that HDA and Ca^{2+} would induce fusion of the outer and inner mitochondrial membranes in the region of contact sites, where the two membranes are close to each other.

Conclusions

Summarizing the data obtained, one can make the following conclusions.

1. The experiments on liposomes showed that, like PA, HDA and TDA are able to induce a Ca^{2+}-dependent permeabilization of liposomes loaded with SRB. One can, therefore, suppose that the Ca^{2+}-dependent, CsA-insensitive pore induced by α,ω-dioic acids in the inner mitochondrial membrane has a lipid nature. At the same time, different kinetics and different concentration dependences of PA/Ca^{2+}- and HDA/Ca^{2+}-induced permeabilization of liposomes and mitochondria suggest that the mechanisms of permeabilization for mono- and dioic fatty acids are also different.

2. Using the method of ultrasound interferometry, we found that HDA/Ca^{2+}-induced permeabilization of liposomes was not accompanied by changes in the phase state of the membrane—in contrast to what was observed in the case of PA/Ca^{2+}-induced permeabilization. Therefore, the mechanism that underlies HDA/Ca^{2+}-induced permeabilization is different from the mechanism of chemotropic phase transition described for PA.

3. Using the method of dynamic light scattering, we revealed that the combined action of HDA and Ca^{2+} resulted in the increase of the hydrodynamic diameter of liposomes, which was apparently accompanied by the formation of short-living lipid pores (fusion pores). It seems that in liver mitochondria, an HDA/Ca^{2+}-induced permeability transition may be underlain by the fusion of the outer and inner mitochondrial membranes, which would result in the formation of fusion pores.

References

Agafonov A, Gritsenko E, Belosludtsev K, Kovalev A, Gateau-Roesch O, Saris N-EL, Mironova GD (2003) A permeability transition in liposomes induced by the formation of Ca^{2+}/palmitic acid complexes. Biochim Biophys Acta 1609:153–160

Agafonov AV, Gritsenko EN, Shlyapnikova EN, Kharakoz DP, Belosludtseva NV, Lezhnev EI, Saris Nils-Erik L, Mironova GD (2007) Ca^{2+}-induced phase separation in the membrane of palmitate-containing liposomes and its possible relation to membrane permeabilization. J Membr Biol 215:57–68

Astashev ME, Belosludtsev KN, Kharakoz DP (2014) Method for digital measurement of phase–frequency characteristics for a fixed length ultrasonic spectrometer. Acoust Phys 60:335–341

Bartlett GR (1959) Phosphorus assay in column chromatography. J Biol Chem 234:466–468

Belosludtsev KN, Belosludtseva NV, Mironova GD (2005) Possible mechanism for formation and regulation of the palmitate-induced cyclosporin A-insensitive mitochondrial pore. Biochemistry (Moscow) 70:815–821

Belosludtsev K, Saris N-E, Andersson LC, Belosludtseva N, Agafonov A, Sharma A, Moshkov DA, Mironova GD (2006) On the mechanism of palmitic acid-induced apoptosis: the role of a pore induced by palmitic acid and Ca^{2+} in mitochondria. J Bioenerg Biomembr 38:113–120

Belosludtsev KN, Belosludtseva NV, Agafonov AV, Astashev ME, Kazakov AS, Saris N-EL, Mironova GD (2014) Ca^{2+}-dependent permeabilization of mitochondria and liposomes by palmitic and oleic acids: a comparative study. Biochim Biophys Acta 1838:2600–2606

Chernomordik LV, Kozlov MM (2003) Protein-lipid interplay in fusion and fission of biological membranes. Annu Rev Biochem 72:175–207

Chernomordik LV, Kozlov MM (2008) Mechanics of membrane fusion. Nat Struct Mol Biol 15:675–683

Di Paola M, Lorusso M (2006) Interaction of free fatty acids with mitochondria: coupling, uncoupling and permeability transition. Biochim Biophys Acta 1757:1330–1337

Dubinin MV, Adakeeva SI, Samartsev VN (2013) Long-chain α, ω-dioic acids as inducers of cyclosporin A-insensitive nonspecific permeability of the inner membrane of liver mitochondria loaded with calcium or strontium ions. Biochemistry (Moscow) 78:412–417

Dubinin MV, Vedernikov AA, Adakeeva SI, Khoroshavina EI, Samartsev VN (2014) Physiological modulators of cyclosporin A-insensitive nonspecific permeability of the inner membrane of liver mitochondria induced by calcium ions and α, ω-hexadecanedioic acid. Biochem (Mosc) Suppl Ser A Membr Cell Biol 8:30–36

Ferdinandusse S, Denis S, Van Roermund C, Wanders RJ, Dacremont G (2004) Identification of the peroxisomal β-oxidation enzymes involved in the degradation of long-chain dicarboxylic acids. J Lipid Res 45:1104–1111

Jackson MB, Chapman ER (2008) The fusion pores of Ca^{2+}-triggered exocytosis. Nat Struct Mol Biol 15:684–689

Kamo N, Muratsugu M, Hongoh R, Kobatake Y (1979) Membrane potential of mitochondria measured with an electrode sensitive to tetraphenylphosphonium and relationship between proton electrochemical potential and phosphorylation potential in steady state. J Membr Biol 49:105–121

Kates M (1972) Techniques of Lipidology. Isolation, analysis and identification of lipids. Elsevier, New York

Kharakoz DP, Panchelyuga MS, Tiktopulo EI, Shlyapnikova EA (2007) Critical temperatures and a critical chain length in saturated diacylphosphatidylcholines: calorimetric, ultrasonic and Monte Carlo simulation study of chain-melting/ordering in aqueous lipid dispersions. Chem Phys Lipids 150:217–228

Kroemer G, Galluzzi L, Brenner C (2007) Mitochondrial membrane permeabilization in cell death. Physiol Rev 87:99–163

Kundu RK, Tonsgard JH, Getz GS (1991) Induction of omega-oxidation of monocarboxylic acids in rats by acetylsalicylic acid. J Clin Invest 88:1865–1872

Lentz BR, Malinin V, Haque ME, Evans K (2000) Protein machines and lipid assemblies: current views of cell membrane fusion. Curr Opin Struct Biol 10:607–615

Malhi H, Guicciardi ME, Gores GL (2010) Hepatocyte death: a clear and present danger. Physiol Rev 90:1165–1194

Markova OV, Bondarenko DI, Samartsev VN (1999) The anion-carrier mediated uncoupling effect of dicarboxylic fatty acids in liver mitochondria depends on the position of the second carboxyl group. Biochemistry (Moscow) 64:565–570

Mironova GD, Gateau-Roesch O, Levrat C, Gritsenko E, Pavlov E, Lazareva AV, Limarenko E, Rey P, Louisot P, Saris N-EL (2001) Palmitic and stearic acids bind Ca^{2+} with high affinity and form nonspecific channels in black-lipid membranes. Possible relation to Ca^{2+}-activated mitochondrial pores. J Bioenerg Biomembr 33:319–331

Mironova GD, Gritsenko E, Gateau-Roesch O, Levrat C, Agafonov A, Belosludtsev K, Prigent A, Muntean D, Dubois M, Ovize M (2004) Formation of palmitic acid/Ca^{2+} complexes in the mitochondrial membrane: a possible role in the cyclosporin-insensitive permeability transition. J Bioenerg Biomembr 36:171–178

Nelson CJ, Otis JP, Martin SL, Carey HV (2009) Analysis of the hibernation cycle using LC-MS-based metabolomics in ground squirrel liver. Physiol Genomics 37:43–51

Orellana M, Rodrigo R, Valdes E (1998) Peroxisomal and microsomal fatty acid oxidation in liver of rats after chronic ethanol consumption. Gen Pharmacol 31:817–820

Papahadjopoulos D, Nir S, Düzgünes N (1990) Molecular mechanisms of calcium-induced membrane fusion. J Bioenerg Biomembr 22:157–179

Rasola A, Bernardi P (2011) Mitochondrial permeability transition in Ca^{2+}-dependent apoptosis and necrosis. Cell Calcium 50:222–233

Reddy JK, Rao MS (2006) Lipid metabolism and liver inflammation. II. Fatty liver disease and fatty acid oxidation. Am J Physiol Gastrointest Liver Physiol 290:852–858

Sanders RJ, Ofman R, Valianpou F, Kemp S, Wanders RJ (2005) Evidence for two enzymatic pathways for omega-oxidation of docosanoic acid in rat liver microsomes. J Lipid Res 46:1001–1008

Sultan A, Sokolove P (2001a) Palmitic acid opens a novel cyclosporin A-insensitive pore in the inner mitochondrial membrane. Arch Biochem Biophys 386:37–51

Sultan A, Sokolove P (2001b) Free fatty acid effects on mitochondrial permeability: an overview. Arch Biochem Biophys 386:52–61

Tonsgard JH (1986) Serum dicarboxylic acids in Reye syndrome. J Pediatr 109:440–445

Wanders RJ, Komen J, Kemp S (2011) Fatty acid omega-oxidation as a rescue pathway for fatty acid oxidation disorders in humans. FEBS J 278:182–194

Wilschut J, Scholma J, Eastman SJ, Hope MJ, Cullis PR (1992) Ca^{2+}-induced fusion of phospholipid vesicles containing free fatty acids: modulation by transmembrane pH gradients. Biochemistry 31:2629–2636

Wojtczak L, Schönfeld P (1993) Effect of fatty acids on energy coupling processes in mitochondria. Biochim Biophys Acta 1183:41–57